Ann. Geophys. Discuss., https://doi.org/10.5194/angeo-2018-50
Manuscript under review for journal Ann. Geophys.
Discussion started: 4 June 2018

Annales Geophysicae Discussions
Open Access
EGU

Turbulent Processes in the Earth's Magnetotail: Spectral and Statistical Research

Liudmyla Kozak[1,2], Bohdan Petrenko[1], Anthony T.Y. Lui[3], Elena Kronberg[4,5], Elena Grigorenko[6], and Andrew Prokhorenkov[1]

[1]Taras Shevchenko National University of Kyiv, Kyiv, Ukraine
[2]Space Research Institute of the National Academy of Sciences of Ukraine and State Space Agency of Ukraine, Kyiv, Ukraine
[3]Johns Hopkins University Applied Physics Laboratory, Laurel MD, USA
[4]Max Planck Institute for Solar System Research, Göttingen, Germany
[5]Department of Earth and Environmental Sciences, Ludwig Maximilian University of Munich, Munich, Germany
[6]Space Research Institute, RAS, Russia

Correspondence: PUT

Abstract. We use the ferroprobe measurements from four spacecraft of Cluster-2 mission (3 events from 2005 to 2015) for the analysis of turbulent processes in the Earth's magnetotail. For this study we conduct the spectral, wavelet and statistical analysis. In the framework of statistical examination, we determine the kurtosis for selected events and conduct extended self-similarity evaluation (analysis of distribution function moments of magnetic field fluctuations on different scales). We compare high order structure function of magnetic fluctuations during dipolarization with isotropic Kolmogorov and three-dimensional log-Poisson model with She-Leveque parameters. We obtain power law scaling of the generalized diffusion coefficient (the power index that varies within the range of $0.2 - 0.7$). The obtained results show the presence of super-diffusion processes. We find the significant difference of the spectral indices for the intervals before and during the dipolarization. Before dipolarization the spectral index lies in the range from -1.68 ± 0.05 to -2.08 ± 0.05 ($\sim 5/3$ according to the Kolmogorov model). During dipolarization the type of turbulent motion changes: on large time-scales the turbulent flow is close to the homogeneous models of Kolmogorov and Iroshnikov-Kraichnan (the spectral index lies in the range $-2.20 \div -1.53$), and at smaller time scales the spectral index is $-2.89 \div -2.35$ (the Hall-MHD model). The kink frequency is less or close to the average value of the proton gyrofrequency.

The wavelet analysis shows the presence of both direct and inverse cascade processes, which indicates the possibility of self-organization processes, as well as the presence of Pc pulsations.

Copyright statement.

1 Introduction

The physical process responsible for the onset of magnetospheric substorms remains an unsolved mystery in spite of more than five decades of intense research efforts after the discovery of this episodic disturbance in the ionosphere and the magnetosphere.

Ann. Geophys. Discuss., https://doi.org/10.5194/angeo-2018-50
Manuscript under review for journal Ann. Geophys.
Discussion started: 4 June 2018

Annales Geophysicae Discussions

Many potential processes have been proposed Nishida and Hones (1974); Rostoker and Eastman (1987); Samson (1998); Rothwell et al. (1988); Lui et al. (1991); Haerendel (1992); Kan (1998); Streltsov et al. (2010). Soon after the turn of the century, two prominent scenarios of substorm development emerged with different emphasis on the initial subsotrm onset location and the associated physical mechanism Baker et al. (1996). The first model is the Near-Earth Neutral Line (NENL) model with the onset location in the middle of the tail at distances of 15-30 Earth radii in which a large-scale process involving reconnection of magnetic field lines is invoked Baker et al. (1996); Nishida (1978). The second one is the Current Disruption (CD) model in which a plasma instability at distances of 6-15 Earth radii is invoked initially Lui (1991); Roux et al. (1991); Samson (1998), followed by magnetic reconnection at further downtail distances Lui (1991). The distinguishing characteristics of these two scenarios are the initial onset location and the associated physical process.

A four-satellite ESA mission, named Cluster-II and a five-satellite NASA mission, named Time History of Events and Macroscale Interactions during Substorms (THEMIS), were launched to identify the location where the substorm disturbances are initiated in the magnetotail Angelopoulos (2008).

The strategy adopted by these missions is to have some satellites situated at different downtail distances to identify the originating location of substorm disturbance. This strategy turns out not to be foolproof as magnetic reconnection was later recognized to be localized in the local time extent and not a large-scale process as originally envisioned Nakamura et al. (2004). Because of the spatial limitation of magnetic reconnection, satellite observations have not led to a compelling conclusion to settle the mystery as observations on the propagation direction of substorm disturbances in the tail yielded diversified results with many reports on results to be consistent with one or the other of the scenarios, i.e., no consistency with one particular model Angelopoulos (2008); Lui (2009); Akasofu (2012, 2017); Panov et al. (2013); Hwang et al. (2014). A complication in distinguishing the two scenarios is the presence of the so-called pseudo-breakups Zelenyi and Veselovskiy (2008); Lopez (1990); Lui (2002, 2004); Runov et al. (2012).

On the other hand, both scenarios have common consequences such as impulsive particle acceleration, dipolarization, and formation of a current wedge Zelenyi and Veselovskiy (2008); Lui (2004). Several plasma instabilities have been proposed to play a role in these substorm scenarios. External and internal plasma environments with the presence of heavy ions affect the occurrence of these instabilities. Instabilities in the CD model includes the ballooning instability Roux et al. (1991); Cheng and Lui (1998) and the cross-field current instability Lui (2004). Although magnetic reconnection is not a plasma instability process, it requires an instability such as ion tearing instability Schindler (1974); Sitnov and Schindler (2010) to form an X-line for its existence. Heavy ions play a significant role in the development of substorms since their presence changes current sheet thickness and its structure, leading to favorable conditions for magnetic reconnection and the generation of Kelvin-Helmholtz instability Kronberg et al. (2014).

Investigation of the magnetotail is significantly complicated by the presence of turbulence due to instability resulting in a “catastrophic” alteration of the flow and magnetic field structure Barenblatt (2004); Frik (1999); Frisch (1995). Complex turbulent processes that occur in the Earth’s magnetosphere cannot be described within the analytical MHD flow models. To consider the properties of turbulence at different temporal and spatial scales, one should adopt methods of statistical physics and the cascade model developed in hydrodynamic theories. Also note that, when considering a statistical system to be characterized

Ann. Geophys. Discuss., https://doi.org/10.5194/angeo-2018-50
Manuscript under review for journal Ann. Geophys.
Discussion started: 4 June 2018

Annales Geophysicae Discussions

by self-similarity, it can be regarded as a physical characteristic of a fractal size equal to the effective Larmor radius of particles and properties of turbulent processes associated not only with the physical mechanisms of instability, but also with symmetries that describe the scale invariance Savin et al. (2011); Chen et al. (2017).

An analytical or numerical solution of the turbulent plasma dynamics (in 3-dimensional geometry) and determination of turbulence features at large time scales are not currently possible. Therefore, statistical properties of turbulence associated with large-scale invariance are determined experimentally along with estimation of spectral indices in the assumption of power laws for plasma parameters. This allows one to get an idea of the physical properties of plasma turbulence and a description of the transport processes in the turbulent regions in qualitative and quantitative terms Kozak et al. (2012); Hadid et al. (2015); Kozak et al. (2015). This approach has yielded important insights on the turbulent plasma characteristics mainly in the magnetosheath. Plasma turbulence in the magnetotail is a key feature for dipolarization in the CD model. The multiscale nature of plasma turbulence at a CD site has also been explored by analysis from the nonlinear dynamics approach or from wave identification Lui and Najmi (1997); Consolini and Lui (1999, 2000); Lui (2002); Consolini (2005); Lui et al. (2008); Yoon et al. (2009); Contel et al. (2009); Zhou et al. (2009); Mok et al. (2010).

In this work, the spectral and statistical approach was carried out to examine the features of the magnetic field dipolarization in the Earth's magnetotail for 3 events (2015-09-12, 2005-10-15, 2005-10-01). The methods and approaches used in the work are described in detail and tested in the works Kozak and Lui (2008); Kozak et al. (2011); Savin et al. (2011); Kozak et al. (2012); Savin et al. (2014); Kozak et al. (2015, 2017); Kronberg et al. (2017). The thermal and energetic characteristics of protons and electrons observed in dipolarization events in 2005 were previously studied in papers by Grigorenko et al. (2016). At the same time, the statistical review provides estimates on the features of turbulent and dynamic processes at small time scales.

2 Used experimental data

The data of the magnetic field for this analysis were obtained by the spacecraft (SC) of the "Cluster-2" mission in the near-Earth tail for 3 events of 2005-2015 during the dipolarization of the magnetic field Fig. 1. The sampling rate is 22.5 Hz. The magnetic field data are obtained by the fluxgate magnetometer (FGM) Balogh et al. (2001). In the course of the study, the peculiarities were considered of the magnetic field fluctuations for moments prior to dipolarization (relative level of fluctuations $\sim 0.05 - 0.24$ (interval 1) and during the dipolarization of the magnetic field (relative fluctuation level $\sim 0.8 - 1$ (interval 2) (Fig. 1). The spacecrafts were at the geocentric distances 11-17 R_E in anti-sunward direction in the pre-midnight sector (Fig. 2).

The event of 2015 satisfies the conditions of dipolarization for the CD model Lui (2018). For the CD model, large magnetic fluctuations predominantly occur around the neutral sheet of the magnetotail where $B_z \gg B_x, B_y$. During CD, the level of magnetic fluctuations dB_z/B_{z_0} can reach the order of one or more, where B_{z_0} is the B_z value before CD onset. This type of events typically lasts for several minutes. The B_z component could become negative, in spite of a strong background positive B_z component from the dipole magnetic field. It is accompanied by particle energization and intense fluctuating electric fields.

Ann. Geophys. Discuss., https://doi.org/10.5194/angeo-2018-50
Manuscript under review for journal Ann. Geophys.
Discussion started: 4 June 2018

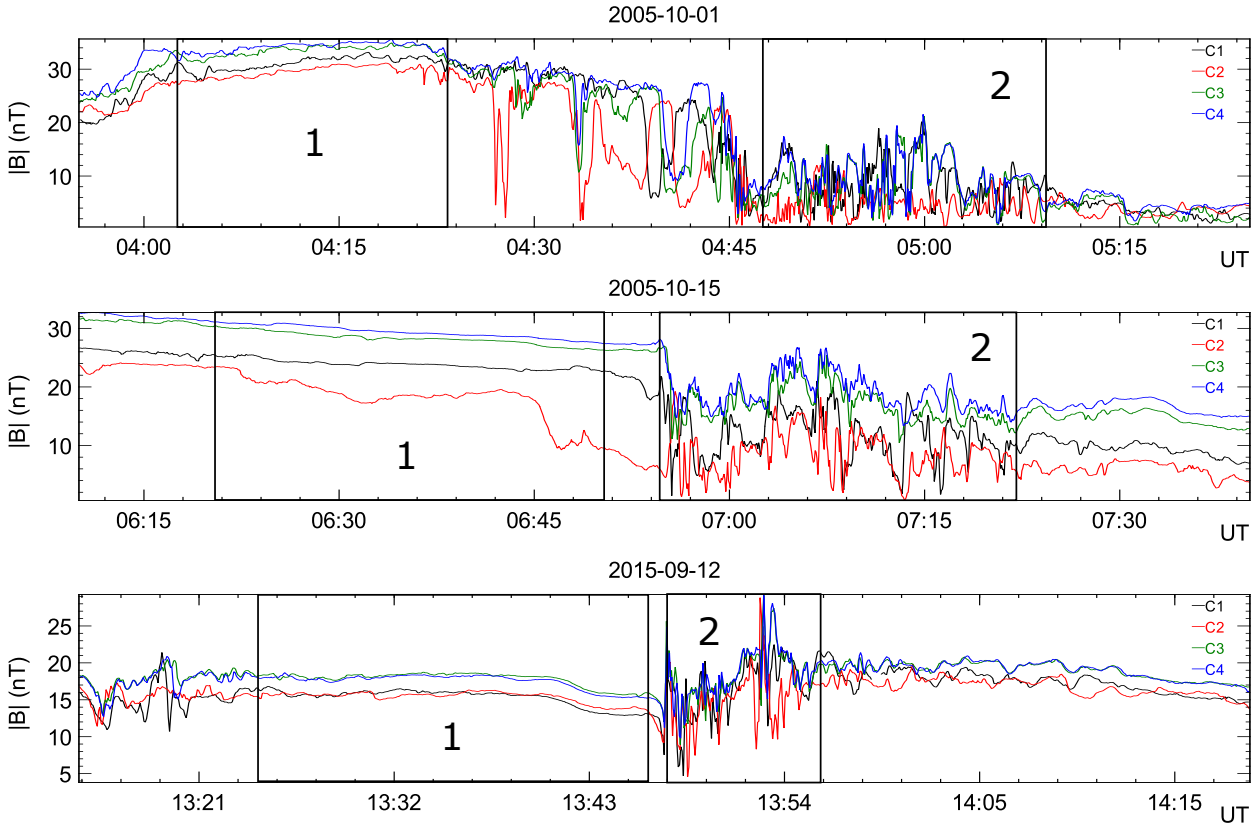

Figure 1. Analyzed fluctuations of magnetic field. 1 — intervals for the moments before dipolarization; 2 — intervals during the dipolarization of the magnetic field.

The cross-tail current breaks up into filaments and may reverse its direction. The associated plasma flow pattern is not organized by the B_z polarity, unlike magnetic reconnection.

In the dipolarization region the fluctuations of magnetic field greatly differ from the region before dipolarization: in particular for event on 2005-10-01 the magnetic field variations normalized to the current mean value are $\delta B_x/B_x \sim 0.5-1$, $\delta B_y/B_y \sim 1$, $\delta B_z/B_z \sim 1$, $\delta B/B \sim 0.8-1$; for event on 2005-10-15 — $\delta B_x/B_x \sim 0.2-0.5$, $\delta B_y/B_y \sim 0.3-1$, $\delta B_z/B_z \sim 0.4-0.8$, $\delta B/B \sim 0.5-1$; for event on 2015-09-12 — $\delta B_x/B_x \sim 0.5-1$, $\delta B_y/B_y \sim 0.5-0.7$, $\delta B_z/B_z \sim 0.8-1$, $\delta B/B \sim 0.8-1$.

Since the region of dipolarization is fixed by four space vehicles, we were able to estimate the speed and direction of the dipolarization front (DF) motion, the thickness of the front (Table 1). The estimated values of plasma characteristics in dipolarization region (interval 2) are collected in Table 2.

Ann. Geophys. Discuss., https://doi.org/10.5194/angeo-2018-50
Manuscript under review for journal Ann. Geophys.
Discussion started: 4 June 2018

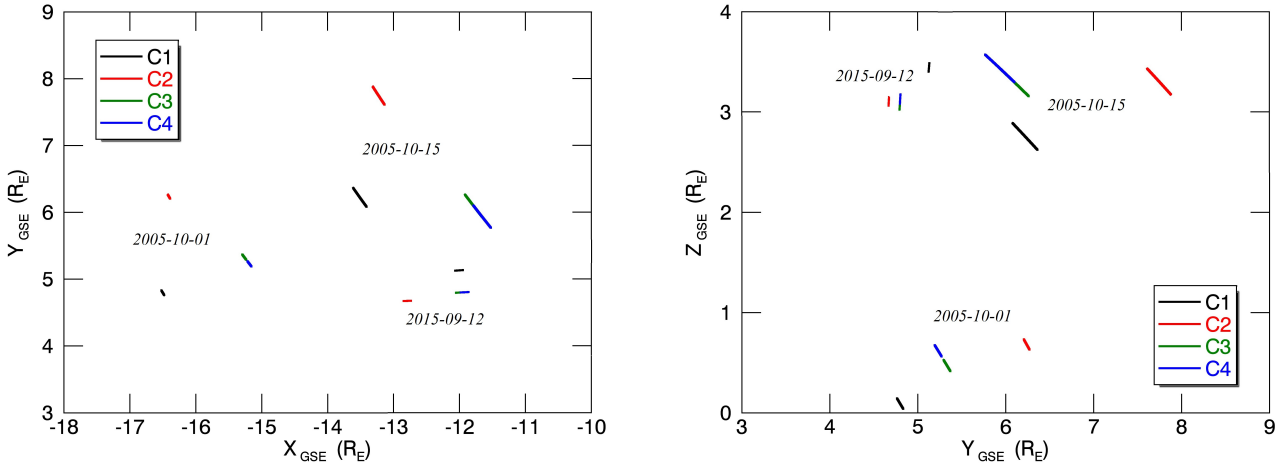

Figure 2. The locations of the satellites

Table 1. Features of the dipolarization fronts (DFs)

		Time of passage of DF	Location			Amplitude of the DF, a, nT	Front duration, b, sec	Standard error of the fitting σ, nT	The speed of the DF, V_{DF}, km/s	The thickness of the DF, d, km
			X_{GSE}, R_E	Y_{GSE}, R_E	Z_{GSE}, R_E					
Fu et al. (2012)						$a > 4$	$b < 8$	$\sigma < 2.5$	210 (to the Earth)	
2015-09-21	C1	13:47:39	-12.0675	5.1244	3.4005	8.89	0.27	1.56		95
	C2	13:47:25	-12.8409	4.6692	3.0676	9.20	0.81	1.08	350 (to	284
	C3	13:47:30	-12.0455	4.7940	3.0293	9.69	2.31	1.29	the Earth)	809
	C4	13:47:31	-11.9729	4.7978	3.0873	9.80	1.77	1.42		620
2005-10-15	C1	06:55:29	-13.4200	6.0945	2.8734	4.59	0.37	3.67		105
	C2	06:56:06	-13.1518	7.6310	3.4116	2.16	0.45	1.08	284 (to	128
	C3	06:56:00	-11.6814	5.9581	3.4140	7.93	3.72	2.13	the Earth)	1056
	C4	06:56:00	-11.5448	5.7908	3.5521	7.54	32.62	1.03		-
2005-10-01	C1	04:44:16	-16.4133	4.6566	0.2978	4.56	0.22	2.09		46
	C2	04:43:28	-16.3271	6.1018	0.8937	4.02	1.33	3.37	208 (to	277
	C3	04:44:19	-15.1508	5.1772	0.6914	9.08	2.81	2.15	the Earth)	584
	C4	04:44:23	-15.0671	5.0758	0.6914	4.53	0.71	1.38		148

Ann. Geophys. Discuss., https://doi.org/10.5194/angeo-2018-50
Manuscript under review for journal Ann. Geophys.
Discussion started: 4 June 2018

Annales Geophysicae Discussions
Open Access
EGU

Table 2. Estimated values of plasma characteristics in dipolarization region

	SC	Average proton-cyclotron frequency $\langle f_{C_p} \rangle$, Hz	Concentration of electrons, n_e, (cm^{-3})	Electron plasma frequency, ω_{pe}, (s^{-1})	Ion plasma frequency, ω_{pi}, (s^{-1})	Electron inertial length, λ_e, (km^{-1})	Ion inertial length, λ_i, (km^{-1})
2015-09-12	C1	0.25	0.25	2.82E+04	6.58E+02	10.63	455.52
	C2	0.22	0.2	2.52E+04	5.89E+02	11.89	509.29
	C3	0.28	0.35	3.34E+04	7.79E+02	8.98	384.99
	C4	0.28	0.2	2.52E+04	5.89E+02	11.89	509.29
2005-10-15	C1	0.19	0.5	3.99E+04	9.31E+02	7.52	322.1
	C2	0.13	0.5	3.99E+04	9.31E+02	7.52	322.1
	C3	0.27	0.5	3.99E+04	9.31E+02	7.52	322.1
	C4	0.3	0.5	3.99E+04	9.31E+02	7.52	322.1
2005-10-01	C1	0.13	0.4	3.57E+04	8.32E+02	8.4	360.12
	C2	0.07	0.4	3.57E+04	8.32E+02	8.4	360.12
	C3	0.14	0.4	3.57E+04	8.32E+02	8.4	360.12
	C4	0.16	0.4	3.57E+04	8.32E+02	8.4	360.12

Moreover, according to Fu et al. (2012), during the dipolarization the variation of B_z for different satellites can be represented as:

$$B_{\text{fit}} = \frac{a}{2}\tanh\left(\frac{\Delta t}{b/2}\right) + \left(c + \frac{a}{2}\right) \tag{1}$$

where, $\Delta t = t - t_{DF}$ represents the interval from 60 s before to 15 s after the dipolarization front. a, b, c are fitting coefficients, and σ is a standard error.

The calculated values of the coefficients are also given in Table 1.

Ann. Geophys. Discuss., https://doi.org/10.5194/angeo-2018-50
Manuscript under review for journal Ann. Geophys.
Discussion started: 4 June 2018

Annales Geophysicae Discussions

3 Results of the Research

3.1 Spectral analysis.

Within the spectral analysis, the spectral power density (PSD) was built from the frequency f, and the power-law dependence $\mathrm{PSD}(f) \sim f^a$ was determined. To determine the PSD signal for a series of N measurements X_n, a discrete Fourier transform Daly and Paschmann (2000) was used:

$$\mathrm{PSD} = \frac{2N}{f_s}\left|\frac{1}{N}\sum_{n=0}^{N-1} X_n \exp\left(\frac{2\pi i n j}{N}\right)\right|^2 \tag{2}$$

where $n = 0, 1 \ldots N-1$, $j = 0, 1 \ldots N/2$.

To find the break points and the slope of the spectrum, we used a piecewise linear approximation of $\log \mathrm{PSD}$ from $\log(f)$ in the frequency range $0.005 - \sim 1.0$ Hz for the pre-dipolarization interval and $0.01 - 3.0$ (events 2005-10-01, 2005-10-15) and $0.01 - 1.0$ (event 2015-09-12) Hz for dipolarization. The limitation of frequencies from above is due to the presence of instrumental noise, and from below, to the amount of data sampling and the edge effect of the smoothing procedure. The PSD results for the absolute value of the magnetic field are shown in Fig. 3 and Table 3.

In the region before the dipolarization (interval 1), for all events considered and spacecraft, there is no sharp change in the PSD power law in the inertial interval (the exponent varies in the range from -2.08 to -1.68). For interval 2 (the dipolarization interval), the situation is significantly different. There is an increase in the "steepness" of PSDs for higher frequencies than the kink frequency, which means more efficient energy transfer from large to smaller scales. For practically all spectra of interval 2, the kink frequency is less or close to the average value of the proton gyrofrequency (Table 2). The kink frequency determines the characteristic frequency of the type change (i.e., the energy transfer rate) of the turbulent cascade in the inertial range. In particular, for events 2015-09-12, 2005-10-15 the break corresponds to about half of the proton frequency $-\omega_c/2$. The fact that the break is observed at frequencies smaller than the proton gyrofrequency may indicate a significant effect of heavy ions at the distances considered. At the same time, the exponent lies in the range of $-2.2 \div -1.53$ on large time scales of $0.01 - \omega_c/2$, and at smaller time scales $\omega_c/2 - 3$ Hz, the value lies in the range $-2.89 \div -2.35$. The greatest difference at different time scales is observed for the 2015 event.

3.2 Wavelet analysis.

Within the framework of the wavelet analysis for a series of measurements X_n ($n = 0, 1 \ldots N-1$) with time shift δt, a Morlet wavelet Torrence and Compo (1998) was used:

$$\Psi_0(\eta) = \pi^{-\frac{1}{4}} e^{i\omega_0 \eta} e^{-\frac{\eta^2}{2}} \tag{3}$$

where ω_0 — dimensionless frequency, η — dimensionless time.

Ann. Geophys. Discuss., https://doi.org/10.5194/angeo-2018-50
Manuscript under review for journal Ann. Geophys.
Discussion started: 4 June 2018

Annales Geophysicae Discussions
Open Access
EGU

Table 3. The results of PSD analysis

Event	SC	Interval 1		Interval 2				
		Slope	Average slope	Kink frequency, f*, Hz	Slope lower f*	Average slope lower f*	Slope higher f*	Average slope lower f*
2015-09-12	C1	-1.7535 ± 0.022	-1.86 ± 0.10	0.14	-1.6340 ± 0.031	-1.59 ± 0.07	-2.8914 ± 0.038	-2.77 ± 0.20
	C2	-1.8758 ± 0.036		0.12	-1.6619 ± 0.034		-2.4966 ± 0.04	
	C3	-1.8722 ± 0.036		0.15	-1.5310 ± 0.042		-2.8527 ± 0.033	
	C4	-1.9552 ± 0.046		0.15	-1.5421 ± 0.044		-2.8473 ± 0.029	
2005-10-15	C1	-1.6800 ± 0.017	-1.86 ± 0.16	0.19	-2.1634 ± 0.020	-2.03 ± 0.33	-2.5265 ± 0.036	-2.50 ± 0.23
	C2	-2.0042 ± 0.019		0.07	-1.5395 ± 0.026		-2.7969 ± 0.016	
	C3	-1.8452 ± 0.023		0.08	-2.1995 ± 0.028		-2.3461 ± 0.023	
	C4	-1.9003 ± 0.045		0.08	-2.1992 ± 0.044		-2.3504 ± 0.047	
2005-10-01	C1	-2.0794 ± 0.034	-2.04 ± 0.04	0.13	-1.6442 ± 0.026	-1.66 ± 0.18	-2.8159 ± 0.045	-2.73 ± 0.16
	C2	-2.0237 ± 0.046		0.07	-1.8831 ± 0.031		-2.4860 ± 0.048	
	C3	-1.9987 ± 0.026		0.08	-1.5828 ± 0.033		-2.8022 ± 0.035	
	C4	-2.0665 ± 0.038		0.1	-1.5261 ± 0.045		-2.8221 ± 0.032	

Ann. Geophys. Discuss., https://doi.org/10.5194/angeo-2018-50
Manuscript under review for journal Ann. Geophys.
Discussion started: 4 June 2018

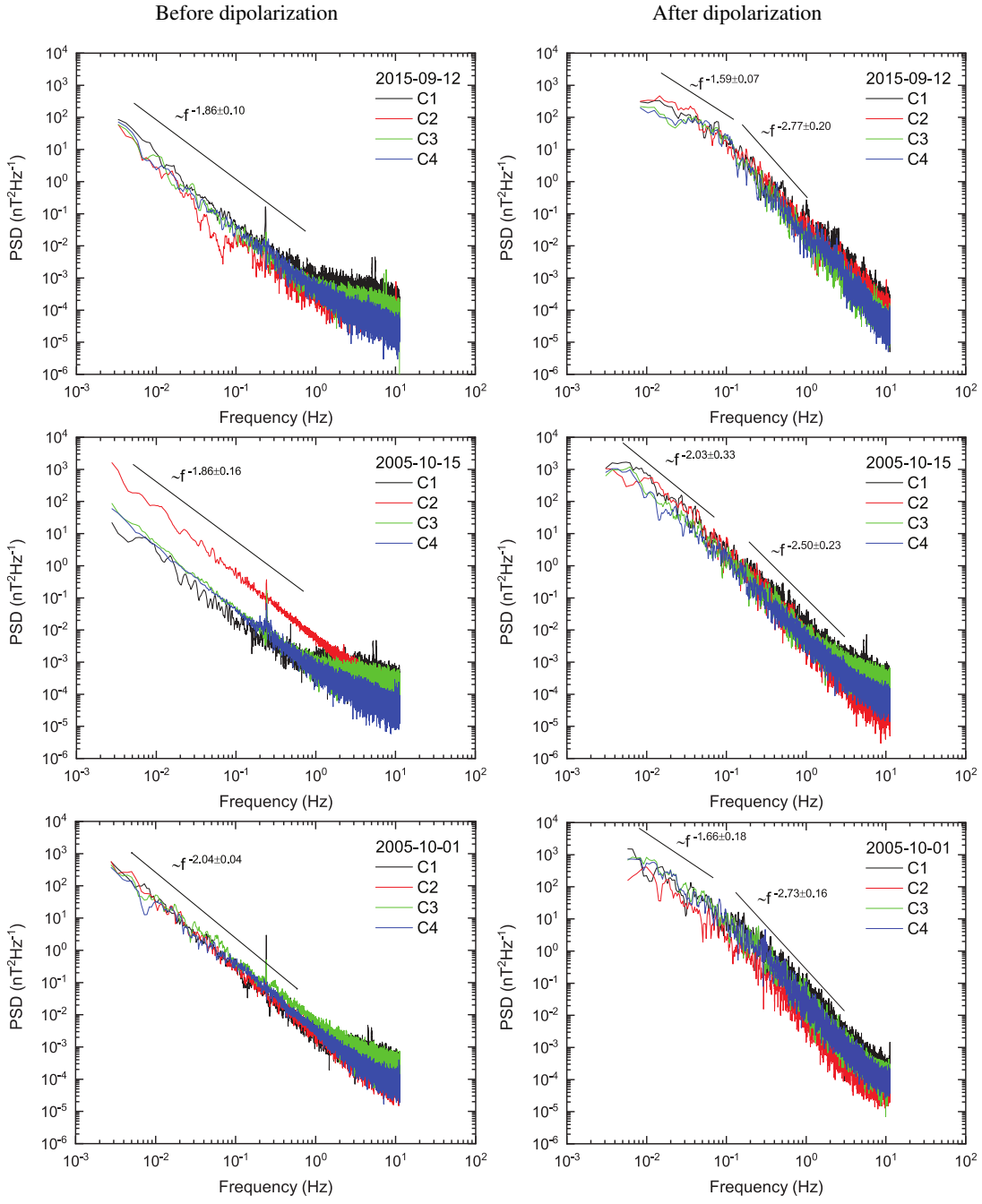

Figure 3. The results of spectral analysis

Ann. Geophys. Discuss., https://doi.org/10.5194/angeo-2018-50
Manuscript under review for journal Ann. Geophys.
Discussion started: 4 June 2018

The continuous wavelet transforms of the discrete signal X_n is defined as the convolution of the mother wavelet whose argument is scaled and transmitted with a signal Farge (1992); Grinsted et al. (2004); Jevrejeva et al. (2003):

$$W_n(s) = \sum_{n'}^{N-1} x_{n'} \Psi^* \left[\frac{(n'-n)\delta t}{s} \right] \tag{4}$$

where $(^*)$ — complex conjugate, $|W_n(s)|^2$ — wavelet power spectrum, s — wavelet scale. Index 0 in Ψ_0 notes that the function is normalized.

The results of the continuous wavelet transform of the magnetic field module in the dipolarization region are shown in Figs. 4 to 6. The time range was chosen to include the dipolarization interval — interval 2 with some margin (± 5 min) to exclude the influence of the edge effects of the wavelet transform to the explored intervals. The upper limit of the wavelet transform is limited by the Nyquist frequency. The sampling frequency of the measurements makes it possible to analyze the presence of high-frequency fluctuations in addition to the low-frequency components.

In Fig. 4 the wavelet analysis of magnetic field module for the event on 2015-09-12 is presented. In this case C3 and C4 were located ahead of the C1 and C2, with C2 being the furthest in the magnetotail. Inverse and direct cascades are present in wavelet analysis at multiple times: 13:47:30 (dipolarization onset) and 13:53:00, both spanning 0.02–0.2 Hz in the frequency domain. This signal broadens for C1 and C2 wavelet and breaks up into smaller time-frequency forms: e.g. the signal on 13:53:00 UT becomes more concentrated in time and frequency domains of 1 minute and 0.01 Hz correspondingly. Wavelet transform for C1 is characterized by a prevalence of intensity enhancements in wide frequency range at an earlier stage of the turbulent phase of dipolarization at 13:47:30-13:50:30 as compared to transforms for C2, C3, C4. Also for C1, it is interesting to note the fact of coexistence of the inverse and direct cascades simultaneously starting at 13:47:30, and wherein the first one lasts for 2 minutes with frequency decreasing from 0.015 Hz to 0.008 Hz and the more intense second one lasts for 2.5 minutes with slight frequency increasing from 0.015 Hz to 0.02 Hz.

Fig. 5 presents the wavelet transform for event 2005-10-15. Taking into account the cone of influence (COI), there are no strong enhancements presented for C3 and C4. For both these satellites, only high-frequency short signals are present. Transformations for C1 and C2 have much richer frequency content. The component 0.008-0.01 Hz is present on all wavelet analysis, with the maximum amplitude shown at the C2 satellite. For C1 this signal has a broader structure, starting from 06:56 until 07:18, with frequency spanning from 0.005 to 0.02 Hz. Both of the satellites hold the same structure of short-term high-frequency signals up to 1 Hz.

Fig. 6 demonstrates the wavelet analysis for event on 2005-10-01. The 3rd and 4th SCs were located relatively close, with 1st and 2nd slightly behind in the magnetotail. Although the onset of dipolarization begins at 04:49, where B_Z component becomes comparable with magnetic field module B, the signal up to this moment is not devoid of high-amplitude changes. Transforms in for C3 and C4, the figures shows strong signals in the frequencies ranging from 0.002 Hz to 0.004 Hz, which span for 10 minutes, with different times for intensity maxima: 04:39 for 3rd SC and 04:42 for 4th. In both cases, a structure of inverse cascade can be traced before dipolarization onset: the frequency decreases from 0.005 to 0.002 Hz. The second inverse cascade lasts for 10 minutes starting from 04:57 in time domain with a gradual decrease in the frequency range from 0.015

Ann. Geophys. Discuss., https://doi.org/10.5194/angeo-2018-50
Manuscript under review for journal Ann. Geophys.
Discussion started: 4 June 2018

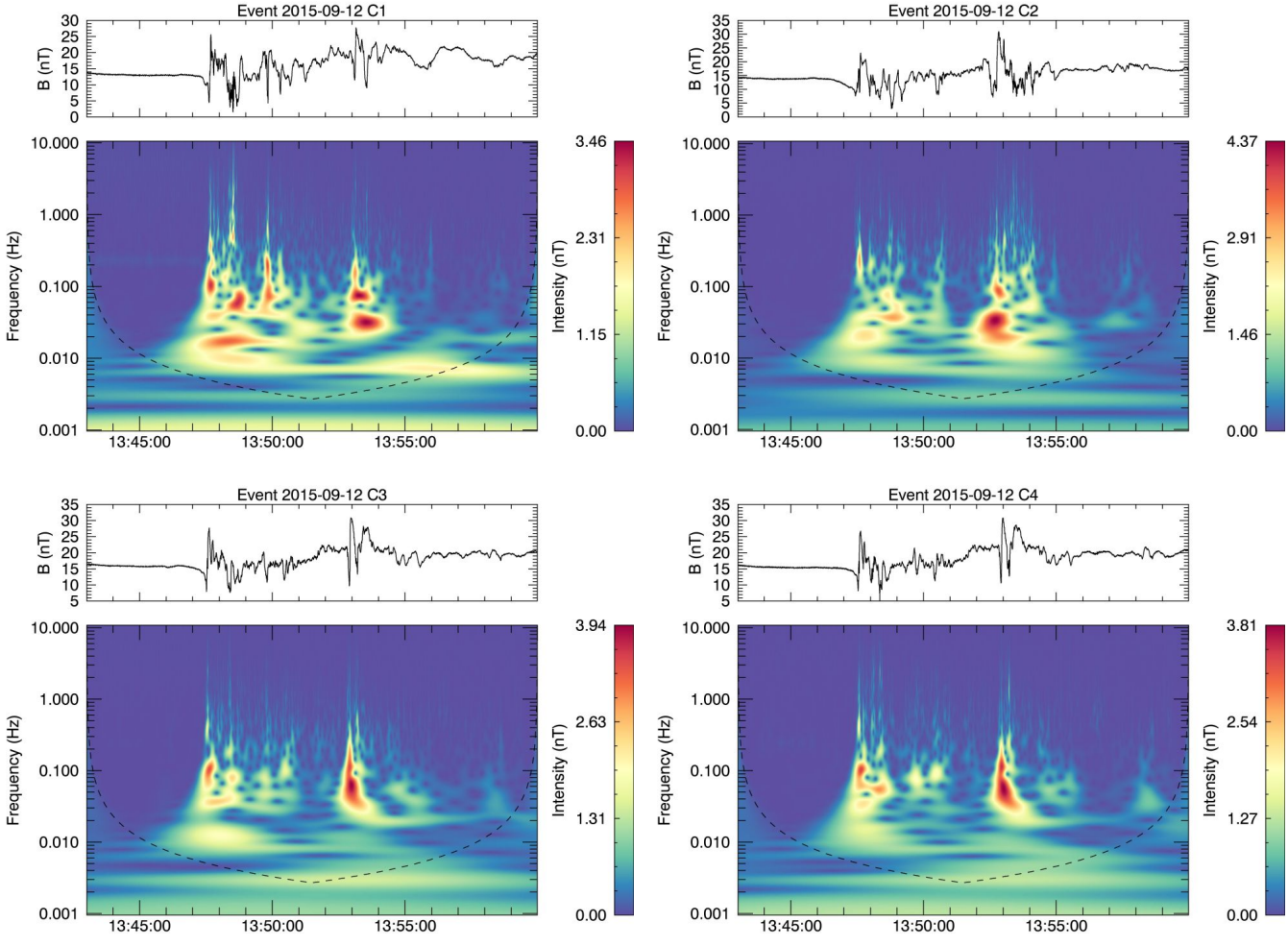

Figure 4. The results of wavelet analysis for event 2015-09-12. The cone of influence is shown by dotted line

to 0.005 Hz, while at higher frequency it breaks up into smaller wave forms. Wavelet decomposition for C2 differs from the others, primarily by the absence of any cascade during the turbulent phase of dipolarization (it is interesting to note that just for this SC the spectral slope of the PSD spectrum is less in absolute value in comparison with other SCs: -2.5 against -2.8) with distinct component on 0.0035 Hz which spans for 8 minutes. The relatively short components, with durations of less than 2 minutes, extend in the frequency range from 0.02 Hz up to 0.2 Hz. For C1 there is a long enhancement at 0.004 Hz, which spans more than 20 minutes, and one with a gradual increase in frequency up to 0.007 Hz, i. e. direct cascade. Such prolonged intensity enhancements are observed with a wide frequency coverage beginning with 0.002 up to 0.01 Hz. A large number of high frequency components appear at both satellite measurement signals.

Ann. Geophys. Discuss., https://doi.org/10.5194/angeo-2018-50
Manuscript under review for journal Ann. Geophys.
Discussion started: 4 June 2018

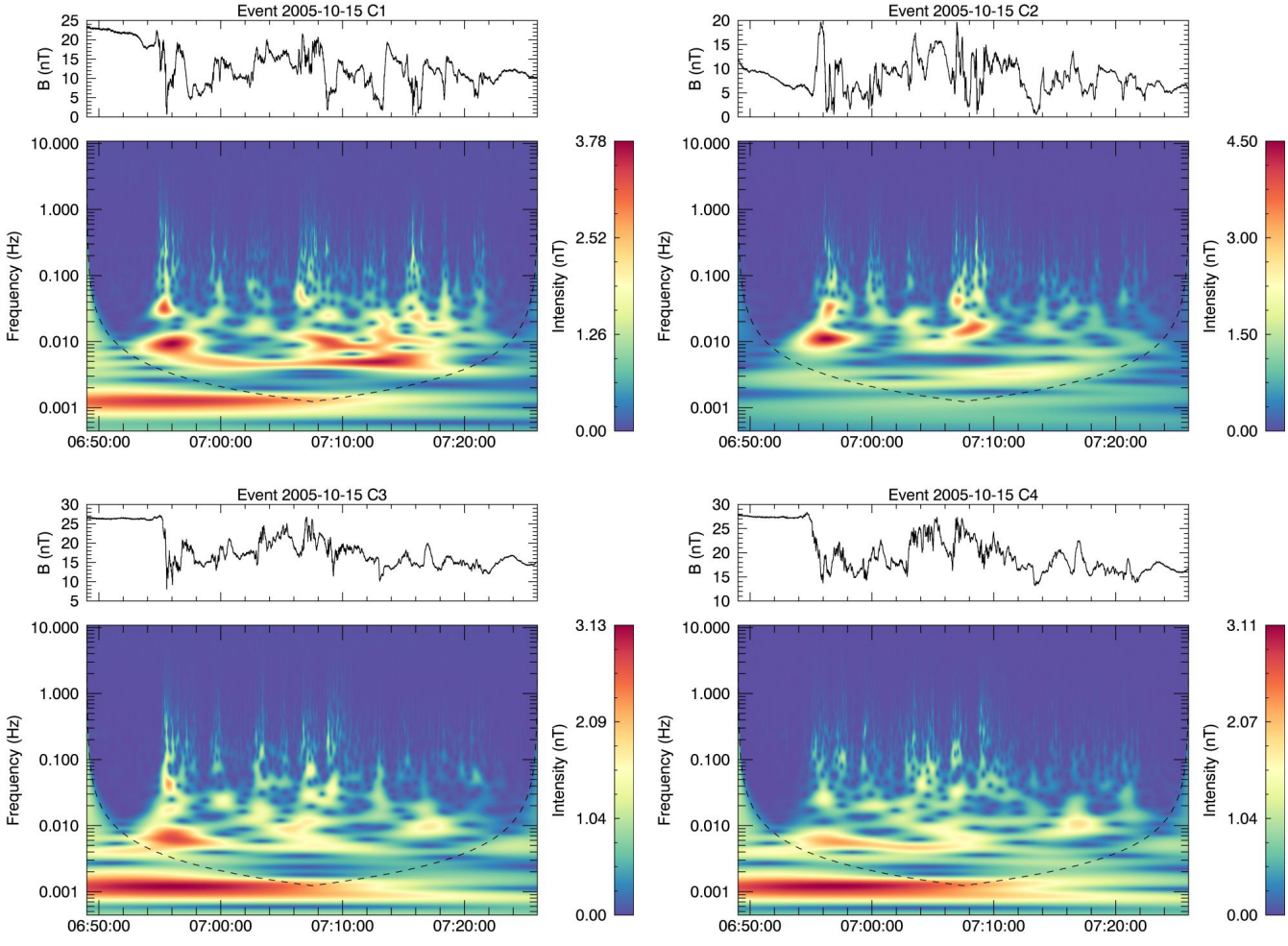

Figure 5. The results of wavelet analysis for event 2005-10-15. The cone of influence is shown by dotted line

Thus, during the dipolarization, the magnetometers of all spacecraft recorded powerful signals with periods of 50, 100, 125, 166, 200 sec, corresponding to Pc4 (45-150 sec) and Pc5 (150-600 sec) pulsations, as well as direct and inverse cascade processes. The presence of inverse cascade processes indicates that together with the decay of the vortex structures, self-organization also takes place, i.e. smaller vortices are grouped into larger vortices. In the analyzed events Pc pulsations are fixed on all satellites — in the spatial range of 11–17 R_E. The largest number of cascade processes is fixed at a distance of 15-16 R_E, and the largest number of inverse cascades is in the range 13-14 R_E.

Ann. Geophys. Discuss., https://doi.org/10.5194/angeo-2018-50
Manuscript under review for journal Ann. Geophys.
Discussion started: 4 June 2018

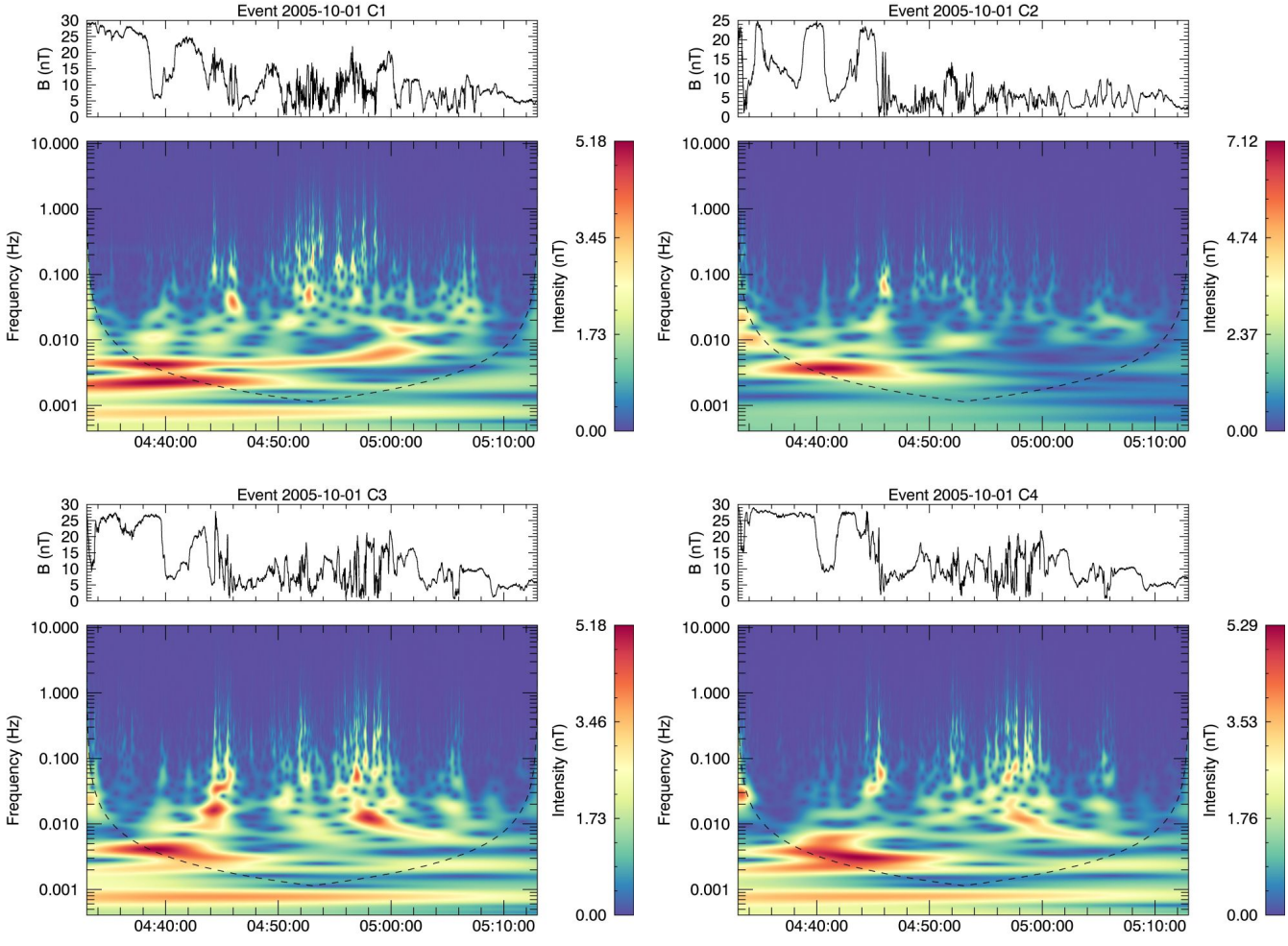

Figure 6. The results of wavelet analysis for event 2005-10-01. The cone of influence is shown by dotted line

3.3 Statistical analysis.

In the presence of intermittency in magnetic field fluctuations, the energy cascade is characterized by non-homogeneous non-linear transfer of energy among smaller and smaller structures, with the result of concentrating the energy on limited regions of space.

This effect becomes more and more intense at smaller and smaller scales. More properly, intermittency corresponds to scale dependent, non-Gaussian, heavy tailed probability distribution functions (PDFs) of the field fluctuations Frisch (1995). Non-Gaussianity of the PDFs, which increases as the scale decreases, is indeed due to the presence of the intense, phase correlated fluctuations, due to the transfer of energy between contiguous eddies. It should be pointed out that spectral properties of the field are not sensitively affected by intermittency. This is normally studied through the scaling properties of PDFs, or through

Ann. Geophys. Discuss., https://doi.org/10.5194/angeo-2018-50
Manuscript under review for journal Ann. Geophys.
Discussion started: 4 June 2018

Annales Geophysicae Discussions
Open Access
EGU

their high order moments (the structure functions), for which models and theoretical results exist Frisch (1995). The observation of intermittency implies that a nonlinear, non-homogeneous energy transfer is going on Zimbardo et al. (2010).

In order to determine the presence of intermittence, an analysis on the value of the excess for all the SCs of the considered events has been performed, as well as the Hölder parameter h for spacecraft C1 has been determined. In this case, the statistical properties of the absolute value of the magnetic field fluctuations at different time scales were analyzed. The use of the Taylor hypothesis for various regions of the magnetospheric tail is detailed in Borovsky, 2003.

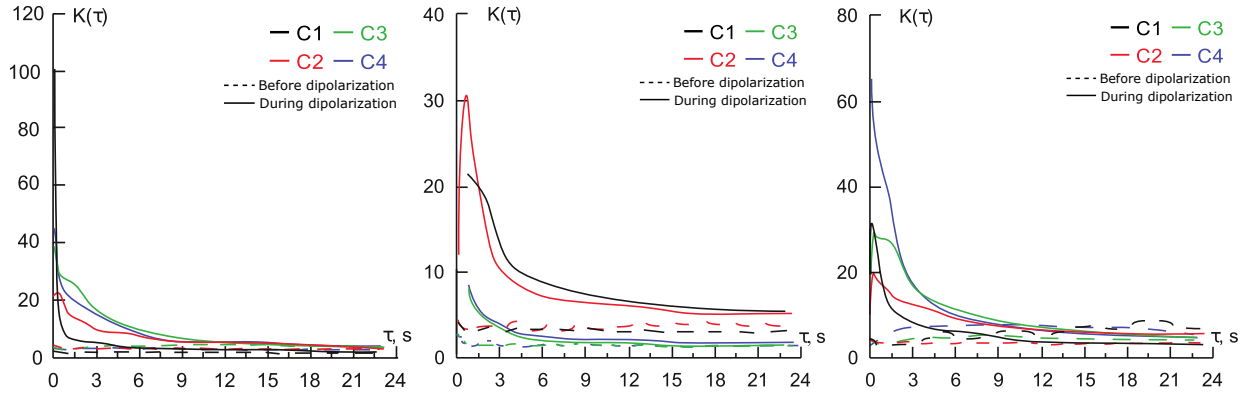

(a) 2015-09-12 (b) 2005-10-15 (c) 2005-10-01

Figure 7. The results of kurtosis

The value of the kurtosis was determined by the moments of the second and fourth order from the formula Zacks (1971):

$$K(\tau) = \frac{S_4(\tau)}{(S_2(\tau))^2} \tag{5}$$

where $S_q(\tau) = \langle |B(t+\tau) - B(\tau)|^q \rangle$ — structure function of q-th order, $\langle \ldots \rangle$ — time average of the data, τ — time scale (time shift), multiple of measurements discretization 0.0445 seconds. When determining the excess value of the magnetic field fluctuations, the dependence of the functions $K(\tau)$ from the scale parameter τ were constructed. The significance of excesses for different mission SC and different events is shown in Fig. 7. It is clearly seen from the graphs that for the interval 1 (dotted line) for almost all satellites the value of $K(\tau)$ varies about 3 (in the range from 5 to 2), which is close to the normal distribution. The only exception is the measurement on the C1 spacecraft for 2005-10-01. Also, for interval 1, spin tone of SC rotation is clearly observed, by sheer accident near the gyrofrequency. For the dipolarization region (interval 2, solid line), the function $K(\tau)$ on small scales varies from 100 (C1, 2015-09-12) to 8 (C3, C4, 2005-10-15).

For SC C3 and C4, changes in the value of kurtosis are very similar. The largest jump is observed for C1, 2015-09-12. A sharp drop in the kurtosis is observed on the scales to the ion-cyclotron frequency Table 2.

The "gap" of values for interval 2 for very small τ can be explained by the instrumental error of observations.

Thus, for a region of dipolarization at small time scales, we have a distribution with a sharper vertex and broad wings (the excess value is greater than 3) than for a normal distribution.

Ann. Geophys. Discuss., https://doi.org/10.5194/angeo-2018-50
Manuscript under review for journal Ann. Geophys.
Discussion started: 4 June 2018

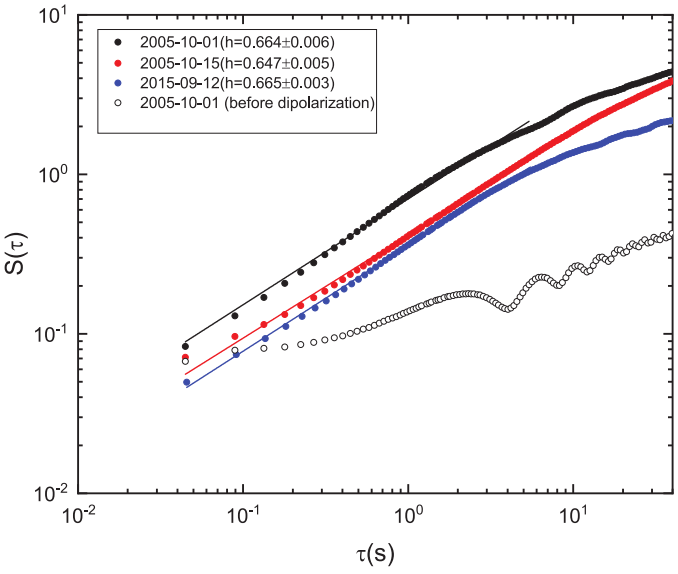

Figure 8. The example of Hölder exponents

The presence of intermittency is indicated by the analysis of the first-order structure function Fig. 8. For a self-affine signal, $S(\tau) \approx \tau^{-h}$, where h is the Hölder exponent ($h = 0.5$ for Brownian motion). The higher value of h afterward indicates a persistent signal with a longer correlation than a random noise and may imply the occurrence of reorganization during dipolarization Chang (1992); Consolini and Lui (2000). In our case, the parameter $h \approx 0.659 \pm 0.005$ at the time of dipolarization.

Also, for the interval prior to dipolarization, the variations "caused" by the presence of spacecraft spin effects in the data are clearly visible.

To compare the type of turbulent processes with the available models of turbulent processes, an analysis of the high-order structural function was done, allowing one to characterize the properties of heterogeneity at small time scales.

In this case, the structural function is determined by the ratio:

$$S_q(\tau) = \langle |B(t+\tau) - B(\tau)|^q \rangle \sim \tau^{\zeta(q)} \tag{6}$$

where $\langle \ldots \rangle$ — time average of the data, τ — time shift.

The existence of the criterion of generalized self-similarity for an arbitrary pair of structural functions $S_q(\tau) \sim S_p(\tau)^{\frac{\zeta(q)}{\zeta(p)}}$ allows one to find $\zeta(q)$ and estimate the type of turbulent and diffusion processes Dubrulle (1994). In this case, the nonlinear functional dependence $\zeta(q)$ from the order of the moment q for experimental data is a consequence of the intermittency of processes. For the interpretation of the nonlinear spectrum $\zeta(q)$, the log-Poisson model of turbulence is used, in which the

Ann. Geophys. Discuss., https://doi.org/10.5194/angeo-2018-50
Manuscript under review for journal Ann. Geophys.
Discussion started: 4 June 2018

power index of the structural function is determined by the relation Dubrulle (1994); She and Leveque (1994); Kozak et al. (2011):

$$\zeta(q) = (1-\Delta)\frac{q}{3} + \frac{\Delta}{1-\beta}\left[1-\beta^{\frac{q}{3}}\right] \tag{7}$$

where β and Δ — parameters that characterize intermittency and singularity of dissipative processes, respectively. It is important to note that within the framework of this model a stochastic multiplicative cascade is considered, and the logarithm of dissipation energy is described by the Poisson distribution. For isotropic three-dimensional turbulence — $\Delta = \beta = 2/3$ (SL) She and Leveque (1994).

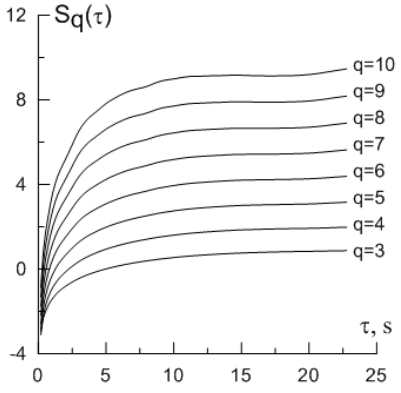

Figure 9. Dependence of order of structure function for different time scales during dipolarization (event 2005-10-15)

The power law of the type $S_q(\tau) \sim \tau^{\zeta(q)}$ (i.e. self-similarity - linear dependence) is observed on limited time scale intervals Fig. 9. For the considered satellite measurements, this interval is close to the value of the ion cyclotron frequency during dipolarization Table 2.

The results of scaling the moments of the probability density function for different orders of q in the analysis of small-scale turbulence and comparing them with the Kolmogorov model are shown in Fig. 10. The results of the ESS analysis of the satellite measurements indicate the heterogeneity of turbulent processes during the dipolarization to describe what can be a log-Poisson cascade model with fitting parameters. The obtained values of the parameters β and Δ are given in Table 4. In addition, the obtained values can be used to determine the characteristics of the diffusion transfer of plasma. The coefficient of generalized diffusion is determined by the parameters of the structural function $\zeta(q)$ (intermittency and singularity) by the relations Chechkin et al. (2008); Treumann et al. (1990); Prokhorenkov et al. (2015):

$$D \propto \tau^R, R = \Delta(1/\beta - 1) \tag{8}$$

This approach is used to estimate the transfer in a statistically inhomogeneous medium, and the index R, in general, is determined by the fractal properties of the medium.

Ann. Geophys. Discuss., https://doi.org/10.5194/angeo-2018-50
Manuscript under review for journal Ann. Geophys.
Discussion started: 4 June 2018

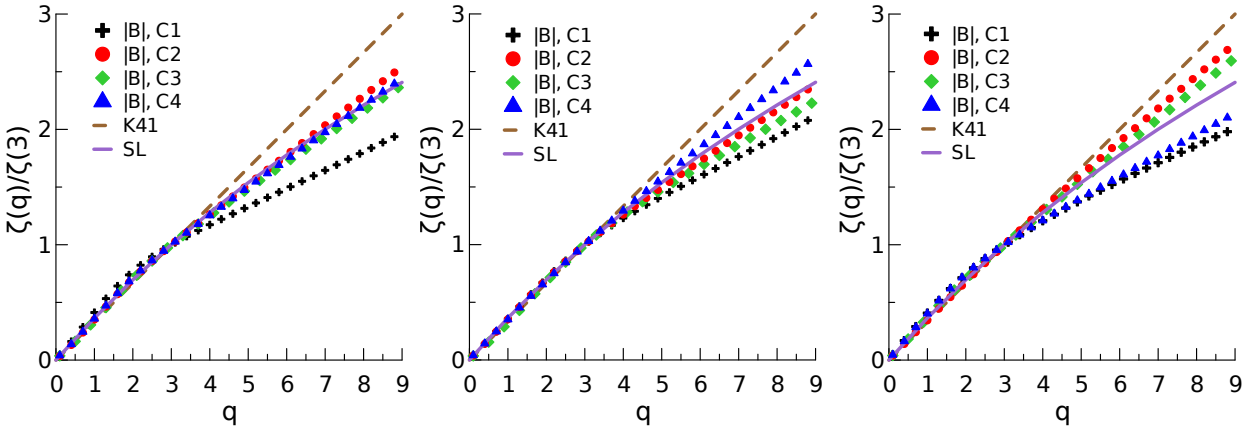

(a) 2015-09-12 (b) 2005-10-15 (c) 2005-10-01

Figure 10. The results of ESS-analysis (during DP). Ratio of the power of the q-th order structural function to the third order function power. The experimental data for the magnetic field are marked with symbol; the solid line corresponds to the value calculated using the formula in the log-Poisson cascade model for $\Delta = \beta = 2/3$ (SL), and the dotted line corresponds to the $q = 3$ (K41)

Table 4. ESS-analysis parameters and diffusion coefficients

Event	SC	β	Δ	$R(-1) = \Delta[1/\beta - 1]$
2015-09-12	C1	0.5 ± 0.029	0.77 ± 0.026	0.77
	C2	0.6 ± 0.018	0.45 ± 0.019	0.30
	C3	0.52 ± 0.091	0.43 ± 0.009	0.40
	C4	0.58 ± 0.016	0.46 ± 0.014	0.33
2005-10-15	C1	0.51 ± 0.015	0.67 ± 0.012	0.64
	C2	0.68 ± 0.025	0.72 ± 0.019	0.34
	C3	0.34 ± 0.027	0.22 ± 0.026	0.43
	C4	0.51 ± 0.026	0.24 ± 0.028	0.23
2005-10-01	C1	0.45 ± 0.015	0.41 ± 0.013	0.5
	C2	0.51 ± 0.013	0.2 ± 0.021	0.2
	C3	0.45 ± 0.024	0.21 ± 0.019	0.26
	C4	0.51 ± 0.026	0.54 ± 0.018	0.52

Ann. Geophys. Discuss., https://doi.org/10.5194/angeo-2018-50
Manuscript under review for journal Ann. Geophys.
Discussion started: 4 June 2018

Annales Geophysicae Discussions
Open Access
EGU

The resulting values of R lie within the range of $0.20 \div 0.77$ (Table 4). Given that the law of particle displacement over time is given by the formula: $\langle \delta x^2 \rangle \propto D\tau \propto \tau^{\delta}$ with an indicator $\delta \propto 1 + R \approx 1.20 \div 1.77 > 1$, this dependence means the existence of super-diffusion.

4 Conclusions

As a result of the analysis, it can be concluded that the relative variations of the magnetic field during the dipolarization exceed the value before dipolarization by more than 5 times. The distribution functions of magnetic field fluctuations during the disruption of the current layer indicate the non-Gaussian statistics of processes, as well as the excess of large-scale perturbations generated by the source.

Comparing the structure functions of the magnetic field fluctuations during dipolarization with Kolmogorov model, it is impossible to describe turbulent processes on small time scales using homogeneous model. Using the coefficients of intermittency and singularity of turbulent processes found in the ESS analysis, the power law of the generalized diffusion coefficient on the scale was obtained (the power index varies within the range of $0.2 - 0.77$), indicating the presence of super-diffusion processes.

One of the important results is the significant difference of the spectral indices for the intervals before and during the dipolarization. Before dipolarization the spectral index lies in the range from -1.68 ± 0.05 to -2.08 ± 0.05 ($\sim 5/3$ according to the Kolmogorov model), and during dipolarization the type of turbulent motions changes: on large time-scales the turbulent flow is close to the to the homogeneous models of Kolmogorov (1941) and Iroshnikov-Kraichnan (1959) (the spectral index lies in the range $-2.20 \div -1.53$), and at smaller time scales the spectral index is $-2.89 \div -2.35$ (the Hall-MHD model). The kink frequency is less or close to the average value of the proton gyrofrequency. The Hall-MHD model includes the Hall term in the magnetic induction equation. The Hall term is proportional to the ion inertial length c/ω_{pi}, which means this term is important for the small scales Galtier and Buchlin (2007). Both the standard MHD and the electron MHD can be recovered from Hall-MHD by taking appropriate limits. By considering magnetic turbulence spectra for scales smaller than c/ω_{pi}, Galtier and Buchlin (2007) found a number of spectral indexes, which go from $\alpha = 7/3$ when magnetic energy dominates kinetic energy, to $\alpha = 11/3$ when kinetic energy dominates magnetic energy.

Also, within the framework of the research the following results were obtained:

- the higher the PSD value, the greater is the value of the height of the excess;
- log-Poisson mode of turbulent processes with She-Leveque parameters corresponds to variations in the value of $K(\tau)$ in the range of $30 - 40$;
- the spectral indices correlate with the values of the diffusion coefficient.

The wavelet analysis showed the presence of both direct and inverse cascade processes, as well as the presence of Pc pulsations. The presence of Pc pulsations in the region of dipolarization was also discussed in Panov et al. (2013, 2015).

Thus, during dipolarization the large-scale and multi-fractal disturbances of the magnetic field are fixed and the presence of inverse cascade processes also indicates the possibility of self-organization processes.

Ann. Geophys. Discuss., https://doi.org/10.5194/angeo-2018-50
Manuscript under review for journal Ann. Geophys.
Discussion started: 4 June 2018

Acknowledgements. The work was conducted in the frame of complex program of National Academy of Science of Ukraine on scientific cosmic researches; with support of education program of Ministry of Education and Science of Ukraine No 2201250 “Education, Training of students, PhD students, scientific and pedagogical staff abroad”; the grant Az. 90 312 from the Volkswagen Foundation (“VW- Stiftung”) and International Institution of Space Research (ISSI-BJ).

We acknowledge Cluster Science Archive (https://www.cosmos.esa.int/web/csa), PI and teams of FGM and CIS instruments for providing the data. The Cluster data used in this study were downloaded from the Cluster Science Archive version 1.2.1 at https://www.cosmos.esa.int/web/csa.

Ann. Geophys. Discuss., https://doi.org/10.5194/angeo-2018-50
Manuscript under review for journal Ann. Geophys.
Discussion started: 4 June 2018

References

Akasofu, S.-I.: Auroral Morphology: A Historical Account and Major Auroral Features During Auroral Substorms, in: Auroral Phenomenology and Magnetospheric Processes: Earth and Other Planets, pp. 29–38, American Geophysical Union, https://doi.org/10.1029/2011gm001156, 2012.

Akasofu, S.-I.: Where is the magnetic energy for the expansion phase of auroral substorms accumulated? 2. The main body, not the magnetotail, Journal of Geophysical Research: Space Physics, 122, 8479–8487, https://doi.org/10.1002/2016ja023074, 2017.

Angelopoulos, V.: The THEMIS Mission, Space Science Reviews, 141, 5–34, https://doi.org/10.1007/s11214-008-9336-1, 2008.

Baker, D. N., Pulkkinen, T. I., Angelopoulos, V., Baumjohann, W., and McPherron, R. L.: Neutral line model of substorms: Past results and present view, Journal of Geophysical Research: Space Physics, 101, 12 975–13 010, https://doi.org/10.1029/95ja03753, 1996.

Balogh, A., Carr, C. M., Acuña, M. H., Dunlop, M. W., Beek, T. J., Brown, P., Fornacon, K.-H., Georgescu, E., Glassmeier, K.-H., Harris, J., Musmann, G., Oddy, T., and Schwingenschuh, K.: The Cluster Magnetic Field Investigation: overview of in-flight performance and initial results, Annales Geophysicae, 19, 1207–1217, https://doi.org/10.5194/angeo-19-1207-2001, 2001.

Barenblatt, G. I.: Turbulent boundary layers at very large Reynolds numbers, Russian Mathematical Surveys, 59, 47, 2004.

Chang, T.: Low-dimensional behavior and symmetry breaking of stochastic systems near criticality-can these effects be observed in space and in the laboratory?, IEEE Transactions on Plasma Science, 20, 691–694, https://doi.org/10.1109/27.199515, 1992.

Chechkin, A. V., Gonchar, V. Y., Gorenflo, R., Korabel, N., and Sokolov, I. M.: Generalized fractional diffusion equations for accelerating subdiffusion and truncated Lévy flights, Physical Review E, 78, https://doi.org/10.1103/physreve.78.021111, 2008.

Chen, C., Fazakerley, A., Khotyaintsev, Y., Lavraud, B., Marcucci, M. F., Narita, Y., Retinò, A., Soucek, J., Vainio, R., Vaivads, A., and Valentini, F.: THOR Exploring plasma energization in space turbulence, Assessment Study Report ESA/SRE, 2017.

Cheng, C. Z. and Lui, A. T. Y.: Kinetic ballooning instability for substorm onset and current disruption observed by AMPTE/CCE, Geophysical Research Letters, 25, 4091–4094, https://doi.org/10.1029/1998gl900093, 1998.

Consolini, G.: On the magnetic field fluctuations during magnetospheric tail current disruption: A statistical approach, Journal of Geophysical Research, 110, https://doi.org/10.1029/2004ja010947, 2005.

Consolini, G. and Lui, A. T. Y.: Sign-singularity analysis of current disruption, Geophysical Research Letters, 26, 1673–1676, https://doi.org/10.1029/1999gl900355, 1999.

Consolini, G. and Lui, A. T. Y.: Symmetry breaking and nonlinear wave-wave interaction in current disruption: Possible evidence for a phase transition, in: Magnetospheric Current Systems, pp. 395–401, American Geophysical Union, https://doi.org/10.1029/gm118p0395, 2000.

Contel, O. L., Roux, A., Jacquey, C., Robert, P., Berthomier, M., Chust, T., Grison, B., Angelopoulos, V., Sibeck, D., Chaston, C. C., Cully, C. M., Ergun, B., Glassmeier, K.-H., Auster, U., McFadden, J., Carlson, C., Larson, D., Bonnell, J. W., Mende, S., Russell, C. T., Donovan, E., Mann, I., and Singer, H.: Quasi-parallel whistler mode waves observed by THEMIS during near-earth dipolarizations, Annales Geophysicae, 27, 2259–2275, https://doi.org/10.5194/angeo-27-2259-2009, 2009.

Daly, P. W. and Paschmann, G.: Analysis Methods for Multi-Spacecraft Data, ISSI Scientific Report SR-001 (Electronic edition 1.1), 2000.

Dubrulle, B.: Intermittency in fully developed turbulence: Log-Poisson statistics and generalized scale covariance, Physical Review Letters, 73, 959–962, https://doi.org/10.1103/physrevlett.73.959, 1994.

Farge, M.: Wavelet Transforms and their Applications to Turbulence, Annual Review of Fluid Mechanics, 24, 395–458, https://doi.org/10.1146/annurev.fl.24.010192.002143, 1992.

Frik, P.: Turbulence: approaches and models, Perm's State Tech. Univ, 1999.

Frisch, U.: Turbulence. The legacy of A. N. Kolmogorov., Cambridge University Press, 1995.

Fu, H. S., Khotyaintsev, Y. V., Vaivads, A., André, M., and Huang, S. Y.: Occurrence rate of earthward-propagating dipolarization fronts, Geophysical Research Letters, 39, https://doi.org/10.1029/2012gl051784, 2012.

Galtier, S. and Buchlin, E.: Multiscale Hall-Magnetohydrodynamic Turbulence in the Solar Wind, The Astrophysical Journal, 656, 560, 2007.

Grigorenko, E. E., Kronberg, E. A., Daly, P. W., Ganushkina, N. Y., Lavraud, B., Sauvaud, J., and Zelenyi, L. M.: Origin of low proton-to-electron temperature ratio in the Earth's plasma sheet, Journal of Geophysical Research: Space Physics, 121, 9985–10,004, https://doi.org/10.1002/2016JA022874, 2016.

Grinsted, A., Moore, J. C., and Jevrejeva, S.: Application of the cross wavelet transform and wavelet coherence to geophysical time series, Nonlinear Processes in Geophysics, 11, 561–566, https://doi.org/10.5194/npg-11-561-2004, 2004.

Hadid, L. Z., Sahraoui, F., Kiyani, K. H., Retinò, A., Modolo, R., Canu, P., Masters, A., and Dougherty, M. K.: Nature of the MHD and Kinetic Scale Turbulence in the Magnetosheath of Saturn: Cassini Observations, The Astrophysical Journal Letters, 813, L29, 2015.

Haerendel, G.: Disruption, ballooning or auroral avalanche-on the cause of substorms, Proc. Int. Conf. on Substorms, Kiruna, Sweden, March 23-27, 1992, pp. 417–420, https://ci.nii.ac.jp/naid/10003640079/en/, 1992.

Hwang, K.-J., Goldstein, M. L., Moore, T. E., Walsh, B. M., Baishev, D. G., Moiseyev, A. V., Shevtsov, B. M., and Yumoto, K.: A tailward moving current sheet normal magnetic field front followed by an earthward moving dipolarization front, Journal of Geophysical Research: Space Physics, 119, 5316–5327, https://doi.org/10.1002/2013ja019657, 2014.

Jevrejeva, S., Moore, J. C., and Grinsted, A.: Influence of the Arctic Oscillation and El Niño-Southern Oscillation (ENSO) on ice conditions in the Baltic Sea: The wavelet approach, Journal of Geophysical Research: Atmospheres, 108, https://doi.org/10.1029/2003jd003417, 2003.

Kan, J. R.: A globally integrated substorm model: Tail reconnection and magnetosphere-ionosphere coupling, Journal of Geophysical Research: Space Physics, 103, 11 787–11 795, https://doi.org/10.1029/98ja00361, 1998.

Kolmogorov, A. N.: Dissipation of Energy in Locally Isotropic Turbulence, Akademiia Nauk SSSR Doklady, 32, 16, 1941.

Kozak, L., Prokhorenkov, A., and Savin, S.: Statistical analysis of the magnetic fluctuations in boundary layers of Earth's magnetosphere, Advances in Space Research, 56, 2091–2096, https://doi.org/10.1016/j.asr.2015.08.009, 2015.

Kozak, L., Lui, A., Kronberg, E., and Prokhorenkov, A.: Turbulent processes in Earth's magnetosheath by Cluster mission measurements, Journal of Atmospheric and Solar-Terrestrial Physics, 154, 115–126, https://doi.org/10.1016/j.jastp.2016.12.016, 2017.

Kozak, L. V. and Lui, A. T.: Statistical analysis of plasma turbulence based on satellite magnetic field measurements, Kinematics and Physics of Celestial Bodies, 24, 209–214, https://doi.org/10.3103/s0884591308040041, 2008.

Kozak, L. V., Pilipenko, V. A., Chugunova, O. M., and Kozak, P. N.: Statistical analysis of turbulence in the foreshock region and in the Earth's magnetosheath, Cosmic Research, 49, 194–204, https://doi.org/10.1134/s0010952511030063, 2011.

Kozak, L. V., Savin, S. P., Budaev, V. P., Pilipenko, V. A., and Lezhen, L. A.: Character of turbulence in the boundary regions of the Earth's magnetosphere, Geomagnetism and Aeronomy, 52, 445–455, https://doi.org/10.1134/s0016793212040093, 2012.

Kraichnan, R. H.: The structure of isotropic turbulence at very high Reynolds numbers, Journal of Fluid Mechanics, 5, 497, https://doi.org/10.1017/s0022112059000362, 1959.

Kronberg, E. A., Ashour-Abdalla, M., Dandouras, I., Delcourt, D. C., Grigorenko, E. E., Kistler, L. M., Kuzichev, I. V., Liao, J., Maggiolo, R., Malova, H. V., Orlova, K. G., Peroomian, V., Shklyar, D. R., Shprits, Y. Y., Welling, D. T., and Zelenyi, L. M.: Circulation of

Heavy Ions and Their Dynamical Effects in the Magnetosphere: Recent Observations and Models, Space Science Reviews, 184, 173–235, https://doi.org/10.1007/s11214-014-0104-0, 2014.

Kronberg, E. A., Grigorenko, E. E., Turner, D. L., Daly, P. W., Khotyaintsev, Y., and Kozak, L.: Comparing and contrasting dispersionless injections at geosynchronous orbit during a substorm event, Journal of Geophysical Research: Space Physics, https://doi.org/10.1002/2016ja023551, 2017.

Lopez, R. E.: Magnetospheric substorms, Johns Hopkins APL Technical Digest, 11, 264–271, 1990.

Lui, A.: Multiscale phenomena in the near-Earth magnetosphere, Journal of Atmospheric and Solar-Terrestrial Physics, 64, 125–143, https://doi.org/10.1016/s1364-6826(01)00079-7, 2002.

Lui, A.: Potential Plasma Instabilities For Substorm Expansion Onsets, Space Science Reviews, 113, 127–206, https://doi.org/10.1023/b:spac.0000042942.00362.4e, 2004.

Lui, A. T. Y.: A synthesis of magnetospheric substorm models, Journal of Geophysical Research: Space Physics, 96, 1849–1856, https://doi.org/10.1029/90ja02430, 1991.

Lui, A. T. Y.: Comment on "Tail Reconnection Triggering Substorm Onset", Science, 324, 1391–1391, https://doi.org/10.1126/science.1167726, 2009.

Lui, A. T. Y.: Review on the Characteristics of the Current Sheet in the Earth's Magnetotail, in: Electric Currents in Geospace and Beyond, pp. 155–175, John Wiley & Sons, Inc., https://doi.org/10.1002/9781119324522.ch10, 2018.

Lui, A. T. Y. and Najmi, A.-H.: Time-frequency decomposition of signals in a current disruption event, Geophysical Research Letters, 24, 3157–3160, https://doi.org/10.1029/97gl03229, 1997.

Lui, A. T. Y., Chang, C.-L., Mankofsky, A., Wong, H.-K., and Winske, D.: A cross-field current instability for substorm expansions, Journal of Geophysical Research, 96, 11 389, https://doi.org/10.1029/91ja00892, 1991.

Lui, A. T. Y., Yoon, P. H., Mok, C., and Ryu, C.-M.: Inverse cascade feature in current disruption, Journal of Geophysical Research: Space Physics, 113, https://doi.org/10.1029/2008ja013521, 2008.

Mok, C., Ryu, C.-M., Yoon, P. H., and Lui, A. T. Y.: Obliquely propagating electromagnetic drift ion cyclotron instability, Journal of Geophysical Research: Space Physics, 115, https://doi.org/10.1029/2009ja014871, 2010.

Nakamura, R., Baumjohann, W., Mouikis, C., Kistler, L. M., Runov, A., Volwerk, M., Asano, Y., Vörös, Z., Zhang, T. L., Klecker, B., Rème, H., and Balogh, A.: Spatial scale of high-speed flows in the plasma sheet observed by Cluster, Geophysical Research Letters, 31, https://doi.org/10.1029/2004gl019558, 2004.

Nishida, A.: Geomagnetic Diagnosis of the Magnetosphere, Springer Berlin Heidelberg, https://doi.org/10.1007/978-3-642-86825-2, 1978.

Nishida, A. and Hones, E. W.: Association of plasma sheet thinning with neutral line formation in the magnetotail, Journal of Geophysical Research, 79, 535–547, https://doi.org/10.1029/ja079i004p00535, 1974.

Panov, E. V., Artemyev, A. V., Baumjohann, W., Nakamura, R., and Angelopoulos, V.: Transient electron precipitation during oscillatory BBF braking: THEMIS observations and theoretical estimates, Journal of Geophysical Research: Space Physics, 118, 3065–3076, https://doi.org/10.1002/jgra.50203, 2013.

Panov, E. V., Wolf, R. A., Kubyshkina, M. V., Nakamura, R., and Baumjohann, W.: Anharmonic oscillatory flow braking in the Earth's magnetotail, Geophysical Research Letters, 42, 3700–3706, https://doi.org/10.1002/2015gl064057, 2015.

Prokhorenkov, A., Kozak, L., Lui, A., and Gala, I.: Diffusion processes in the transition layer of the Earth's magnetosphere, Advances in Astronomy and Space Physics, 2015.

Rostoker, G. and Eastman, T.: A boundary layer model for magnetospheric substorms, Journal of Geophysical Research, 92, 12 187, https://doi.org/10.1029/ja092ia11p12187, 1987.

Rothwell, P. L., Block, L. P., Silevitch, M. B., and Fälthammar, C. G.: A new model for substorm onsets: The pre-breakup and triggering regimes, Geophysical Research Letters, 15, 1279–1282, https://doi.org/10.1029/gl015i011p01279, 1988.

Roux, A., Perraut, S., Robert, P., Morane, A., Pedersen, A., Korth, A., Kremser, G., Aparicio, B., Rodgers, D., and Pellinen, R.: Plasma sheet instability related to the westward traveling surge, Journal of Geophysical Research, 96, 17 697, https://doi.org/10.1029/91ja01106, 1991.

Runov, A., Angelopoulos, V., and Zhou, X.-Z.: Multipoint observations of dipolarization front formation by magnetotail reconnection, Journal of Geophysical Research: Space Physics, 117, https://doi.org/10.1029/2011ja017361, 2012.

Samson, J. C.: Nonlinear, Hybrid, Magnetohydrodynamic Instabilities Associated with Substorm Intensifications Near the Earth, in: Substorms-4, pp. 505–509, Springer Netherlands, https://doi.org/10.1007/978-94-011-4798-9_104, 1998.

Savin, S., Budaev, V., Zelenyi, L., Amata, E., Sibeck, D., Lutsenko, V., Borodkova, N., Zhang, H., Angelopoulos, V., Safrankova, J., Nemecek, Z., Blecki, J., Buechner, J., Kozak, L., Romanov, S., Skalsky, A., and Krasnoselsky, V.: Anomalous interaction of a plasma flow with the boundary layers of a geomagnetic trap, JETP Letters, 93, 754–762, https://doi.org/10.1134/s0021364011120137, 2011.

Savin, S., Amata, E., Budaev, V., Zelenyi, L., Kronberg, E. A., Buechner, J., Safrankova, J., Nemecek, Z., Blecki, J., Kozak, L., Klimov, S., Skalsky, A., and Lezhen, L.: On nonlinear cascades and resonances in the outer magnetosphere, JETP Letters, 99, 16–21, https://doi.org/10.1134/s002136401401010x, 2014.

Schindler, K.: A theory of the substorm mechanism, Journal of Geophysical Research, 79, 2803–2810, https://doi.org/10.1029/ja079i019p02803, 1974.

She, Z.-S. and Leveque, E.: Universal scaling laws in fully developed turbulence, Physical Review Letters, 72, 336–339, https://doi.org/10.1103/physrevlett.72.336, 1994.

Sitnov, M. I. and Schindler, K.: Tearing stability of a multiscale magnetotail current sheet, Geophysical Research Letters, 37, https://doi.org/10.1029/2010gl042961, 2010.

Streltsov, A. V., Pedersen, T. R., Mishin, E. V., and Snyder, A. L.: Ionospheric feedback instability and substorm development, Journal of Geophysical Research: Space Physics, 115, https://doi.org/10.1029/2009ja014961, 2010.

Torrence, C. and Compo, G. P.: A Practical Guide to Wavelet Analysis, Bulletin of the American Meteorological Society, 79, 61–78, https://doi.org/10.1175/1520-0477(1998)079<0061:apgtwa>2.0.co;2, 1998.

Treumann, R. A., Brostrom, L., LaBelle, J., and Sckopke, N.: The plasma wave signature of a “magnetic hole” in the vicinity of the magnetopause, Journal of Geophysical Research, 95, 19 099, https://doi.org/10.1029/ja095ia11p19099, 1990.

Yoon, P. H., Lui, A. T. Y., and Bonnell, J. W.: Identification of plasma instability from wavelet spectra in a current disruption event, Journal of Geophysical Research: Space Physics, 114, https://doi.org/10.1029/2008ja013816, 2009.

Zacks, S.: The theory of statistical inference., Wiley, 1971.

Zelenyi, L. M. and Veselovskiy, I. S.: Space geoheliophysics, vol. 1, Phyzmatlit, 2008.

Zhou, M., Ashour-Abdalla, M., Deng, X., Schriver, D., El-Alaoui, M., and Pang, Y.: THEMIS observation of multiple dipolarization fronts and associated wave characteristics in the near-Earth magnetotail, Geophysical Research Letters, 36, https://doi.org/10.1029/2009gl040663, 2009.

Zimbardo, G., Greco, A., Sorriso-Valvo, L., Perri, S., Vörös, Z., Aburjania, G., Chargazia, K., and Alexandrova, O.: Magnetic Turbulence in the Geospace Environment, Space Science Reviews, 156, 89–134, https://doi.org/10.1007/s11214-010-9692-5, 2010.